

EXPERIMENTAL CHARACTERIZATION AND OPTIMIZATION OF HIGH-BRIGHTNESS ELECTRON BEAM AT THE NSLS SDL

X. Yang, J. B. Murphy, H. Qian, S. Seletskiy, Y. Shen, and X. J. Wang,
National Synchrotron Light Source, BNL, Upton, NY 11973, U.S.A.

Abstract

The Source Development Laboratory (SDL) at the National Synchrotron Light Source (NSLS) is a laser linac facility dedicated for laser seeded FEL and beam physics R&D. The SDL consists of a RF synchronized Ti:sapphire laser, a BNL photocathode RF gun, a four-magnet chicane bunch compressor, and a 300 MeV linac. To further improve the performance of the laser seeded FEL at the NSLS SDL, we have carried out a systematic experimental characterization of the high-brightness electron beam generated by the photocathode RF gun. We will present the experimental studies of transverse emittance of electron beam as a function of RF gun phase and solenoid magnet for electron beam charge ranging from 350 pC to 1 nC.

charge emittance compensation solenoid magnet developed in the Brookhaven National Laboratory (BNL) [1,2], a transverse normalized rms emittance of 4 mm·mrad with 1nC of bunch charge was obtained.

Optimization of operating parameters of the RF gun, such as the laser injection phase and the space-charge compensation are required for the generation of a high-brightness electron beam. We have carried out a systematic experimental characterization of the transverse emittance of electron beam as a function of RF gun phase and solenoid magnet for electron beam charge ranging from 350 pC to 1 nC.

EXPERIMENTAL SETUP

The SDL accelerator features a 6MeV BNL gun, two SLAC-type traveling-wave accelerating structures providing 70MeV followed by a 4 dipole chicane and three more accelerating structures with a final energy of up to 250MeV [3]. A spectrometer dipole after the last structure enables energy spectra and time resolved measurements [4]. The RF gun consists of a half cell and a full cell. A magnesium cathode is located on the side of the half cell. A single solenoid magnet is mounted at the exit of the RF gun to compensate for the transverse emittance growth due to the space-charge effect.

The beam transverse emittance was measured downstream of the 4th accelerating structure with a standard quadrupole scan technique. The beam size was measured on a YAG crystal downstream of a quadrupole magnet which was varied so that the beam passed and a data translation 8-bit frame grabber both synchronized

INTRODUCTION

Small transverse emittance, high peak current, and small energy spread are keys for achieving high energy gains in the seeded FEL experiments. The electrons with a small energy spread and low space-charge-induced emittance are emitted from the photocathode surface with a strong RF field (~100MV/m). The quick acceleration of the electron beam in a photoinjector prevents thermalization of the beam's phase space. However, the emittance growth, due to the RF and the space-charge effects, occurs in the RF gun. In particular, the transverse emittance increases close to the cathode surface due to transverse defocusing space-charge force. We use a spatial laser shaping to produce a nearly flat-topped charge density electron beam, and a 9ps long Gaussian laser pulse to reduce the longitudinal space charge force. As an example, after a 1.6-cell RF gun with a space-

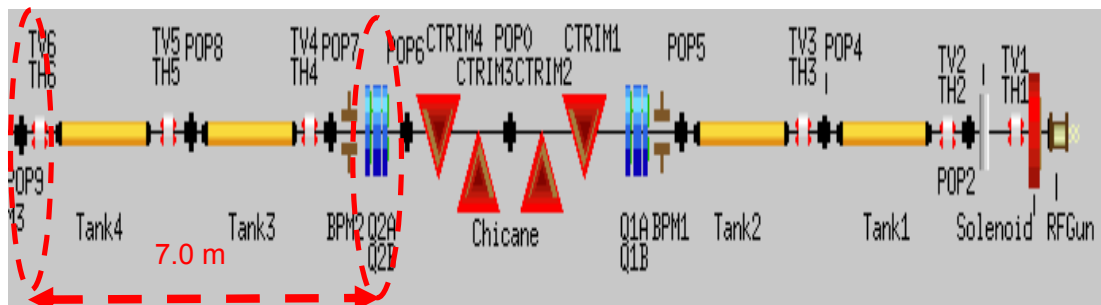


Figure 1: Schematic diagram of the experimental arrangement.

to the electron beam for a single-shot measurement. The combination of a polarizer and a half-wave plate was used to increase the dynamic range of the CCD camera. The beam waist of a 1nC bunch on the YAG screen can be as small as ~ 10 pixels before the image saturates. The resolution on the CCD camera was achieved to be $24.1\mu\text{m}/\text{pixel}$.

The beam size on a screen at a distance L from a quadrupole is given by Eq. (1):

$$x = x_{\min} \sqrt{1 + \left(\frac{L}{x_{\min}}\right)^4 \left(\frac{\varepsilon_{un}}{f_w}\right)^2 \left(1 - \frac{f_w}{f}\right)^2} \quad (1)$$

where ε_{un} is the un-normalized rms emittance, f is the quadrupole's focal length, and f_w is the focal length producing the minimum spot size x_{\min} [5]. Longer the drift distance L is, larger the range of spot size variation on the YAG screen is. So we chose the quadrupole and YAG screen pair indicated by red dash ellipses in Fig. 1 to measure the emittance, the drift distance is 7.04m. The beam size at each quadrupole setting is measured by averaging 5 different images. The image is truncated outside the manual bounding box. Gaussian fit is applied to the intensity histogram of the image, and the background level is set to 1.5 sigma. After applying the background subtraction to the image, the first and second integrated moments are calculated. The transport matrix from the quadrupole to YAG screen is calculated based upon the quadrupole setting and the drift distance. Based upon the measured sigma matrix at YAG screen and the transport matrix, the initial sigma matrix is obtained by least square fit [6].

MEASUREMENTS

The quantum efficiency and the electron charge in the bunch were measured as a function of the laser injection phase on a charge monitor downstream of the solenoid magnet and upstream of the linac, as shown in Fig. 2. The laser injection phase is the RF phase when the center of a laser pulse arrives at the cathode surface. The data was taken at a constant laser energy of $11.9\mu\text{J}$ and a cathode field of $\sim 105\text{MV}/\text{m}$. The laser spot size at the cathode was fixed to 2mm in diameter. The solenoid field was fixed at 1.91kG. When the laser injection phase is smaller than 70° , the data agrees very well with the fitted curve using Eq. (2) [7]:

$$QE = a \times \left(\hbar\omega - W_0 + b\sqrt{\beta E \sin \theta} \right) \quad (2)$$

where QE is the quantum efficiency, $\hbar\omega$ is the photon energy, $W_0=3.66\text{eV}$ is the work function of the Mg cathode

at zero field, $E \approx 105\text{MV}/\text{m}$ is the peak electric field on the axis at the cathode, β is the field enhancement factor, and a and b are material-dependent fitting parameters. Eq. (2) is obtained in the case that quantum efficiency is dominated by the Schottky effect. However, we observed a sharp drop on the bunch charge when the laser injection phase was above 73° . This can be explained by the charge loss in beam transport due to a significant decrease in beam energy when the laser injection phase is above 70° .

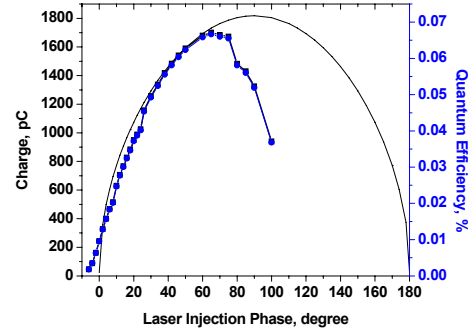


Figure 2: Electron charge and quantum efficiency as a function of laser injection phase.

Inside the RF gun, the beam is dominated by the space-charge effect. However, the transverse emittance growth due to the linear space-charge effect can be compensated with an optimal solenoid magnetic field. The horizontal emittance vs. the solenoid field at a bunch charge of $\sim 300\text{pC}$ is shown in Fig. 3. The red and blue curves are the data taken before and after the cathode cleaning respectively. There was a factor of ~ 2.5 improvement on the transverse emittance after the cathode cleaning. Also, we observed a factor of ~ 10 improvement on quantum efficiency after the cathode cleaning. The data shown in Fig. 2 is after the cathode cleaning. In both cases, the optimal solenoid fields were $\sim 1.47\text{kG}$.

In order to investigate the contribution to the emittance growth due to the RF field in the gun, we measured the normalized transverse emittance as a function of the laser injection phase at the optimal solenoid field of 1.47kG. Laser energy was varied in the measurement in order to keep the charge constant. Emittance measurements were carried out at three different charges of 300pC, 500pC, and 1nC, and they are shown in Fig. 4 as the black, red, and green curves respectively.

Since the charge was kept constant at each measurement, the contribution to the emittance growth due to the space-charge effect was constant. The RF-induced emittance growth starts to increase with the laser injection phase when it's above 30° . The emittance grows faster when the bunch charge increases.

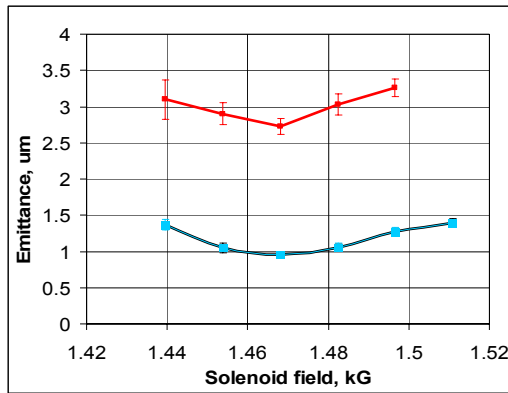


Figure 3: Normalized rms transverse emittance as a function of solenoid magnetic field at the bunch charge of $\sim 300\text{pC}$ and laser injection phase of 25° . The red and blue curves are the data taken before and after the cathode cleaning respectively.

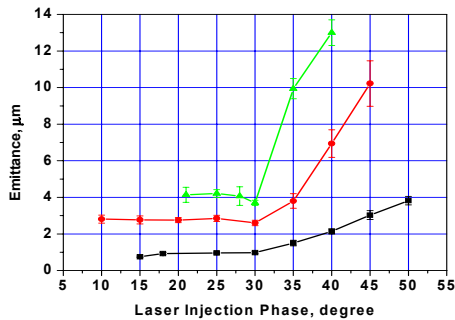


Figure 4: Normalized rms transverse emittance as a function of laser injection phase for constant solenoid field and constant charge at 300pC (black), 500pC (red), and 1nC (green).

CONCLUSIONS

The transverse emittance was investigated experimentally for high brightness electron beam generation. The transverse emittance growth due to the RF and the space charge effects in the RF gun were measured as functions of the laser injection phase. Normalized rms transverse emittances of $1\mu\text{m}$, $2.8\mu\text{m}$, and $4\mu\text{m}$ are achieved at the charge of 300pC , 500pC , and 1nC respectively when the solenoid field is set at the optimal.

Comparing the cases before and after the cathode cleaning, we observed a factor of ~ 10 improvement on quantum efficiency, and a factor of ~ 2.5 improvement on the transverse emittance.

We will upgrade the frame grabber from 8-bit to 12-bit to improve the image resolution, and also investigate the uncertainty of the emittance measurement.

ACKNOWLEDGEMENT

The authors would like to thank B. Podobedov for useful discussions and Pooran Singh for technical support.

REFERENCES

- [1] D. T. Palmer et al, Proc. Particle Accelerator Conf., Canada, 1997, p. 2687.
- [2] X. J. Wang and I. Ben-Zvi, Proc. Particle Accelerator Conf., Canada, 1997, p. 2793.
- [3] W. S. Graves et al, Proc. Particle Accelerator Conf., Chicago, June 2001, p.2860.
- [4] W. S. Graves et al, Proc. Particle Accelerator Conf., Chicago, June 2001, p.2224.
- [5] B. E. Carlsten et al, Nucl. Instr. and Meth. A 331 (1993) 791.
- [6] H. Loos, Manual: "The SDL control Software Package".
- [7] J. Yang et al, Jpn. J. Appl. Phys., Vol. 44, No. 12 (2005).